PREPARED FOR THE U.S. DEPARTMENT OF ENERGY,
UNDER CONTRACT DE-AC02-76CH03073

PPPL-3598
UC-70

PPPL-3598

Enhancement of Mode-converted Electron Bernstein Wave Emission during NSTX H-mode Plasmas

by

G. Taylor, P.C. Efthimion, B. Jones, B.P. LeBlanc, and R. Maingi

August 2001

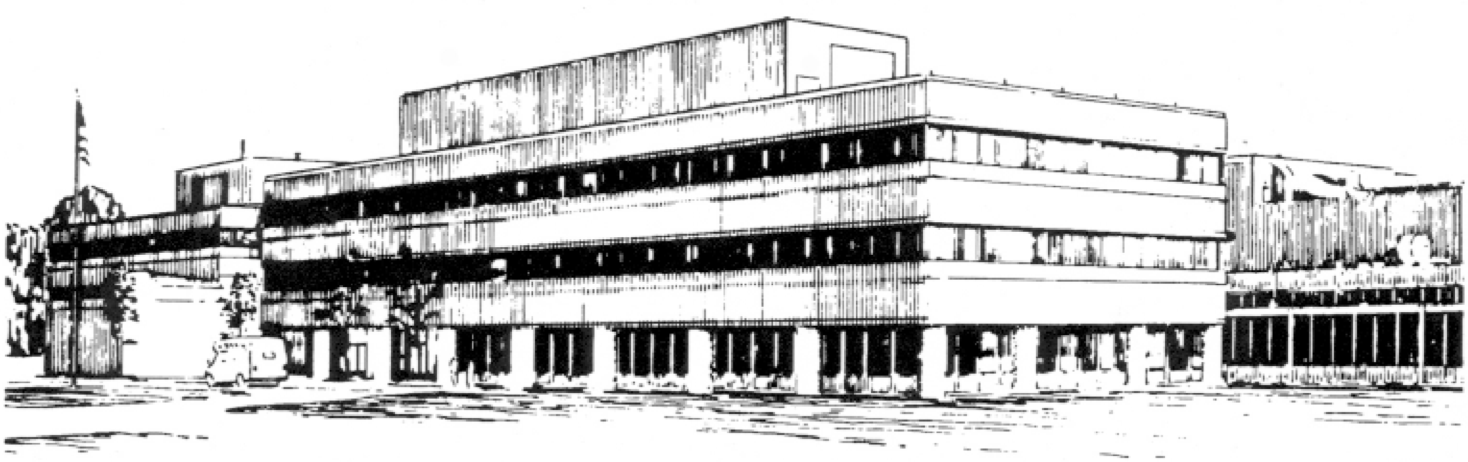

PRINCETON PLASMA PHYSICS LABORATORY
PRINCETON UNIVERSITY, PRINCETON, NEW JERSEY

ENHANCEMENT OF MODE-CONVERTED ELECTRON BERNSTEIN WAVE EMISSION DURING NSTX H-MODE PLASMAS

G. Taylor, P.C. Efthimion, B. Jones, B.P. LeBlanc
Princeton Plasma Physics Laboratory, Princeton, New Jersey 08543

R. Maingi
Oak Ridge National Laboratory, Oak Ridge, Tennessee 08731

Abstract

A sudden, threefold increase in emission from fundamental electrostatic electron Bernstein waves (EBW) which mode convert and tunnel to the electromagnetic X-mode has been observed during H-mode transitions on the NSTX spherical torus plasma. The mode-converted EBW emission viewed normal to the magnetic field on the plasma midplane increases when the density profile steepens in the vicinity of the mode conversion layer, which is located in the plasma scrape off. The measured conversion efficiency during the H-mode is consistent with the calculated EBW to X-mode conversion efficiency derived using edge density data. Calculations indicate that there may also be a small residual contribution to the measured X-mode electromagnetic radiation from polarization-scrambled, O-mode emission, converted from EBWs.

PACS# 52.55.Fa, 52.35.Hr

I. INTRODUCTION

Abrupt transitions to a high energy and particle confinement (H-mode) regime [1] have now been reported on several spherical torus (ST) plasma devices [2-4]. Because of their improved confinement characteristics, H-mode plasmas offer the possibility of more efficient cost effective nuclear fusion reactors. ST plasma devices, such as NSTX [5], are characterized by relatively high electron densities (1 - 5 $\times 10^{19} m^{-3}$) and low confining magnetic fields (< 0.6T), so that the electron plasma frequency normally far exceeds the electron cyclotron frequency. As a result, fundamental and low harmonic electron cyclotron emission (ECE) cannot propagate in ST plasmas, so that diagnostic and heating techniques that rely on ECE cannot be used. Electron Bernstein waves (EBW) can readily propagate in ST plasmas, they have no high density cutoffs and they exhibit strong absorption at the electron cyclotron resonances [6]. These properties make EBWs potentially attractive as a tool for measuring local electron temperature and for local electron heating and current drive for ST plasmas. However, EBWs cannot propagate beyond the upper hybrid resonance (UHR) that surrounds an ST plasma. There are two potential EBW conversion processes to electromagnetic modes that can be employed to indirectly access the EBW emission inside the plasma. The first process involves the conversion of EBWs to the slow X-mode at the UHR [6-8]. The left hand cutoff of the slow X-mode, the UHR, and the right hand cutoff of the fast X-mode form a cutoff-resonance-cutoff triplet allowing the slow X-mode to tunnel through the UHR to the fast X-mode. In this paper we will refer to this as B-X mode conversion. The maximum B-X conversion efficiency for $k_{//}=0$ is given by [6]:

$$C_{\max} = 4e^{-\pi\eta}\left(1-e^{-\pi\eta}\right) \qquad (1)$$

where η is the tunneling parameter. For magnetic scale lengths much greater than the density scale length at the UHR [6]:

$$\eta \approx \left[\omega_{ce} L_n / c\alpha\right]\left(\sqrt{1+\alpha^2}-1\right)^{1/2} \qquad (2)$$

$$\text{where:} \quad \alpha = \left[\omega_{pe}/\omega_{ce}\right]_{UHR} \quad \text{and} \quad L_n = \left|\frac{n_e}{dn_e/dR}\right|_{UHR}$$

Here ω_{ce} and ω_{pe} are the electron cyclotron frequency and electron plasma frequency, respectively, n_e is the electron density and c is the velocity of light. As can be seen from equations (1) and (2), the B-X mode conversion efficiency is very sensitive to the electron density scale length at the UHR layer where the mode conversion and tunneling occurs. On NSTX, the maximum mode conversion efficiency typically occurs for L_n~ 0.5-1 cm.

The second mode conversion process requires the coincidence of the X-mode and O-mode cutoffs [9-13]. This process, referred to here as B-X-O mode conversion, has been previously studied on Wendelstein 7-AS [14,15] and requires an oblique view of the plasma at a specific angle. The B-X-O emission leaves the plasma through an angular window with a transmission function given by [11,13]:

$$T(N_{\perp}, N_{//}) = \exp\left\{-\pi k_o L_n \sqrt{(Y/2)}\left[2(1+Y)(N_{//,opt} - N_{//})^2 + N_{\perp}{}^2\right]\right\} \qquad (3)$$

where: $N_{//,opt}^2 = [Y/(Y+1)]$, $Y = (\omega_{ce}/\omega)$, ω_{ce} is evaluated at the cutoff and ω is the wave frequency. For typical NSTX plasma parameters, this B-X-O emission window is located at about ±35° from the antenna axis in the toroidal direction. As shown in equation (3), the emission window has a width that depends on L_n at the X-mode and O-mode cutoffs. It can also potentially contribute to the measured X-mode emission if there is polarization scrambling of the O-mode emission resulting from reflections.

The natural steepening of the edge density gradient that occurs at the L to H transition can enhance the conversion and tunneling efficiency of both the B-X and B-X-O conversion processes if the steepening occurs in the vicinity of the EBW mode conversion layer. On NSTX, the relevant UHR for fundamental EBW B-X mode conversion normally lies in the scrape off region near the last closed flux surface, so the edge density steepening during the H-mode might be expected to enhance the EBW conversion efficiency.

This paper reports the observation of enhanced fundamental B-X mode conversion efficiency during neutral-beam-heated NSTX H-mode plasmas with an axial magnetic field of 0.45 T [4]. The effective conversion efficiency was obtained from the ratio of the absolutely calibrated mode-converted EBW emission radiation temperature (T_{rad}) to the electron temperature (T_e) measured by laser Thomson scattering. T_{rad}/T_e was compared to the theoretical B-X conversion efficiency calculated from equation (1) using edge density data from laser Thomson scattering. Recently, enhancements in B-X-O emission have also been observed during H-mode discharges in the MAST ST device at Culham, England [3]. Section II of this paper describes the experimental setup for the EBW emission measurements, section III presents an example of the EBW emission data during H-mode plasmas and section IV presents an analysis of these data and a discussion.

II. EXPERIMENTAL SETUP

Mode-converted EBW emission was measured with a broadband, polarizing antenna which viewed the NSTX plasma through a vacuum window on the horizontal midplane. The antenna was oriented to collect predominantly X-mode emission during the plasma current flat top. The antenna was connected to a fast frequency scanning, 12-18 GHz, heterodyne radiometer [16]. 12-18 GHz emission corresponds to non-Doppler shifted fundamental EBW radiation emitted from a region which extends from a major radius of 0.75 to 1.1 m on the horizontal midplane of NSTX, for an axial magnetic field of 0.45 T. The EBW emission spectrum in this band was measured every 100μs. The Shafranov-shifted axis was at about 0.9 m during these experiments, so this emission is expected to come from the core of the NSTX plasma. EBW radiation temperatures quoted in this paper were derived from an absolute calibration of the 12-18 GHz radiometer with a chopped 77K blackbody source. The magnetic field profile used to map emission data from frequency to major radius was obtained from EFIT equilibria. The emission data were mapped to major radius assuming that the emission is non-Doppler shifted fundamental EBW emission.

III. MEASUREMENT OF EBW EMISSION DURING H-MODES

Figure 1 shows the evolution of major plasma parameters for a NSTX discharge which exhibits a L-H transition at 0.2 s and an H-mode phase which lasts 60 ms (shown shaded). Figure 1(a) shows the evolution of the plasma current which reaches a flat top of 1 MA at 0.18 s. 1 MW of neutral beam heating was injected from 0.1 to 0.26 s (Fig. 1(b)). The deuterium wall recycling (Fig. 1 (c)) decreases suddenly at about 0.2 s marking the L-H transition. Figure 1(d) shows the T_{rad} of 16 GHz mode-converted fundamental EBW emission, measured by the EBW radiometer. Immediately before the L-H transition the EBW T_{rad} is 50 eV. At the L-H transition the EBW T_{rad} suddenly increases to 150 eV. Through the H-mode phase the deuterium recycling gradually increases, while the EBW T_{rad} gradually decreases until the collapse of the H-mode at 0.26 s when the EBW emission becomes negligible. Thomson scattering electron density and temperature profiles were acquired at the three times of interest, A, B and C (indicated by vertical dashed lines in Fig. 1). Time A is well before the H-mode when the measured EBW T_{rad} is only a few eV, time B is just before the L-H transition when T_{rad} has increased to 50 eV and time C is during the H-mode when T_{rad} is 120 eV.

Figure 2 shows the EBW spectrum mapped to major radius for the three times of interest marked in Fig. 1. An approximate threefold increase in EBW emission occurs at all measured frequencies between time B and C. The vertical dashed line in Fig. 2 indicates the source location of the 16 GHz emission shown in Fig. 1, this location lies close to the magnetic axis and the peak of the emission spectrum at time B and C.

Figure 3 shows the electron density profile at the three times of interest marked in Fig.1. The location of the last closed flux surface is indicated by a vertical dashed line and the relevant density for mode conversion of 16 GHz EBW emission is indicated by the gray horizontal line. B-X mode conversion for this emission frequency occurs at $n_e = 2.4 \times 10^{18}\ m^{-3}$ which lies in the scrape off, just outside the last closed flux surface. The edge density profile in the vicinity of the mode conversion location steepens significantly during the H-mode phase of the discharge.

IV. ANALYSIS OF MODE-CONVERTED EBW EMISSION

The measured 16 GHz EBW T_{rad}, which maps to a major radius of 0.87 m, was compared to the T_e measured by Thomson scattering at the three times of interest shown in Fig. 1. T_{rad}/T_e was taken to be a measure of the EBW mode conversion efficiency, this efficiency is plotted versus time into the discharge in Fig. 4 (filled circles). The errors in T_e are relatively small so the error bars on T_{rad}/T_e are largely due to uncertainties in calibrating and mapping the EBW T_{rad}. Since the UHR lies in the NSTX scrape off an exponential fit was applied to the Thomson scattering edge density data in Fig. 3 to yield L_n at the UHR. These L_n values were used in equation (1) to calculate C_{max}, which is plotted as open circles in Fig.4. It should be noted that there is an additional phase factor that results from the interference of the inward and outward going components of the slow X-mode [6] and this can reduce the tunneling efficiency between the slow and fast X-mode. The fluctuations in T_{rad}, plotted in Fig 1(d), may be caused by this interference or by electron density fluctuations in the vicinity of the UHR. During the H-mode phase of the discharge, when L_n =1.5 cm, the measured T_{rad}/T_e is 11%, higher than the calculated B-X mode conversion efficiency of 8%, but within the relatively large uncertainties in the calculated B-X mode conversion efficiency. The exponential dependence on L_n in the expression for the B-X mode conversion efficiency (eq. (1)) leads to large uncertainties in the calculated efficiencies plotted in Fig. 4. At the two times before the H-mode, L_n is 2-3 times larger than during the H-mode, as a result the calculated B-X conversion efficiency is negligible at these times. B-X-O mode conversion may also contribute to the EBW radiometer signal if there is polarization scrambling of the O-mode emission due to reflections. Evidence for substantial depolarization due to reflections has already been noted during experiments with a similar antenna on CDX-U [16]. The maximum contribution from B-X-O conversion was calculated by combining the B-X-O angular emission window from equation (3) with the measured antenna pattern. The B-X-O conversion, with complete depolarization, could provide an additional T_{rad}/T_e~3% at time C, so that the combined total conversion efficiency (plotted as open squares in Fig. 4) is in good agreement with the measured T_{rad}/T_e during the H-mode. At the two times before the H-mode there is also reasonable agreement between the measured and calculated mode conversion efficiencies if depolarized B-X-O emission is assumed to contribute to the measured emission. It should be noted that ray tracing analyses of EBW rays that lie within the acceptance angle of the antenna indicate that there can be significant Doppler shifts for rays at the edge of the antenna pattern. These Doppler shifts can significantly refract EBWs contributing to a low level of non-local emission that might be expected to dominate the measured EBW emission at low measured conversion efficiencies (< 5%).

The natural steepening that occurs in the edge density profile during H-modes is observed to significantly improve the coupling efficiency between EBWs and electromagnetic modes outside the plasma, and confirms the EBW mode conversion physics. However, the 10-15% mode conversion efficiency measured during NSTX H-modes is insufficient in itself to justify the implementation of mode-converted EBW heating or current drive schemes, which require much higher (>50%) conversion efficiencies to be viable. Since the fundamental EBW mode conversion layer lies outside the last closed flux surface it may be possible to increase the B-X conversion efficiency by imposing a steepened scrape off density by means of a local limiter. Experiments to investigate this possibility are presently being conducted on CDX-U and initial results are encouraging [17].

ACKNOWLEDGEMENTS

This work was supported by US Department of Energy contract no. DE-AC02-76CH03073 and by a US Department of Energy research grant which is part of a program to encourage innovations in magnetic fusion energy diagnostic systems.

REFERENCES

[1] F. Wagner, *et al*., Phys. Rev. Lett. **49**, 1408 (1982).
[2] A. Sykes, *et al*., Phys. Rev. Lett. **84**, 495 (2000).
[3] A. Sykes, J.W. Ahn, R. Akers, et al., Physics of Plasmas **8**, 2101 (2001)
[4] R. Maingi, M.G. Bell, R.E. Bell, *et al*., "Observations of First H-mode Transitions in NSTX", Princeton Plasma Physics Laboratory Report PPPL-3563, submitted to Phys. Rev. Lett. (2001).
[5] M. Ono, *et al*., Proc. 17th IAEA Fus. Energy Conf. (IAEA, Vienna, 1999), Vol. 3, p. 1135.
[6] A.K. Ram and S.D. Schultz, Physics of Plasmas **7**, 4084 (2000).
[7] S. Nakajima and H. Abe, Phys. Rev. A **38**, 4373 (1988).
[8] H. Sugai, Phys. Rev. Lett. **47**, 1899 (1981).
[9] J. Preinhaelter and V. Kopécky, J. Plasma Phys. **10**, 1 (1973).
[10] H. Weitzner and D.B. Batchelor, Phys. Fluids **22**, 1355 (1979).
[11] E. Mjølhus, J. Plasma Phys. **31**, 7 (1984).
[12] S. Nakajima and H. Abe, Phys. Lett. A **124**, 295 (1987).
[13] F.R. Hansen, *et al.*, J. Plasma Phys. **39**, 319 (1988).
[14] H.P. Laqua, *et al*., Phys. Rev. Lett. **78**, 3467 (1997).
[15] H.P. Laqua, *et al*., Phys. Rev. Lett. **81**, 2060 (1998).
[16] G. Taylor, P.C. Efthimion, B. Jones, *et al*., Rev. Sci. Instrum. **72**, 285 (2001).
[17] G.Taylor, P.C. Efthimion, B. Jones, *et al*., "Electron Bernstein Wave Research on CDX-U and NSTX", Proceedings of 14th Topical RF Conf., (Oxnard, Calif., May 2001)

FIGURE CAPTIONS

Figure 1

Evolution of EBW emission during a NSTX discharge with an H-mode transition. Time dependence of (a) the plasma current, (b) the neutral beam power, (c) the deuterium recycling light and (d) 16 GHz fundamental mode-converted EBW emission from the plasma core.

Figure 2

Fundamental mode converted EBW emission mapped to major radius for the three times of interest marked in Fig. 1, namely, 0.164, 0.197 and 0.230 s.

Figure 3

Electron density profiles, measured by laser Thomson scattering for the three times of interest marked in Fig. 1.

Figure 4

Measured and calculated mode conversion efficiency for 16 GHz EBW emission at the three times of interest shown in Fig. 1. The solid circles are the measured EBW mode conversion efficiency, the open circles are the calculated maximum B-X EBW conversion efficiency and the open squares are the calculated maximum EBW conversion efficiency, including B-X and B-X-O conversion and assuming complete depolarization of the B-X-O emission due to reflections.

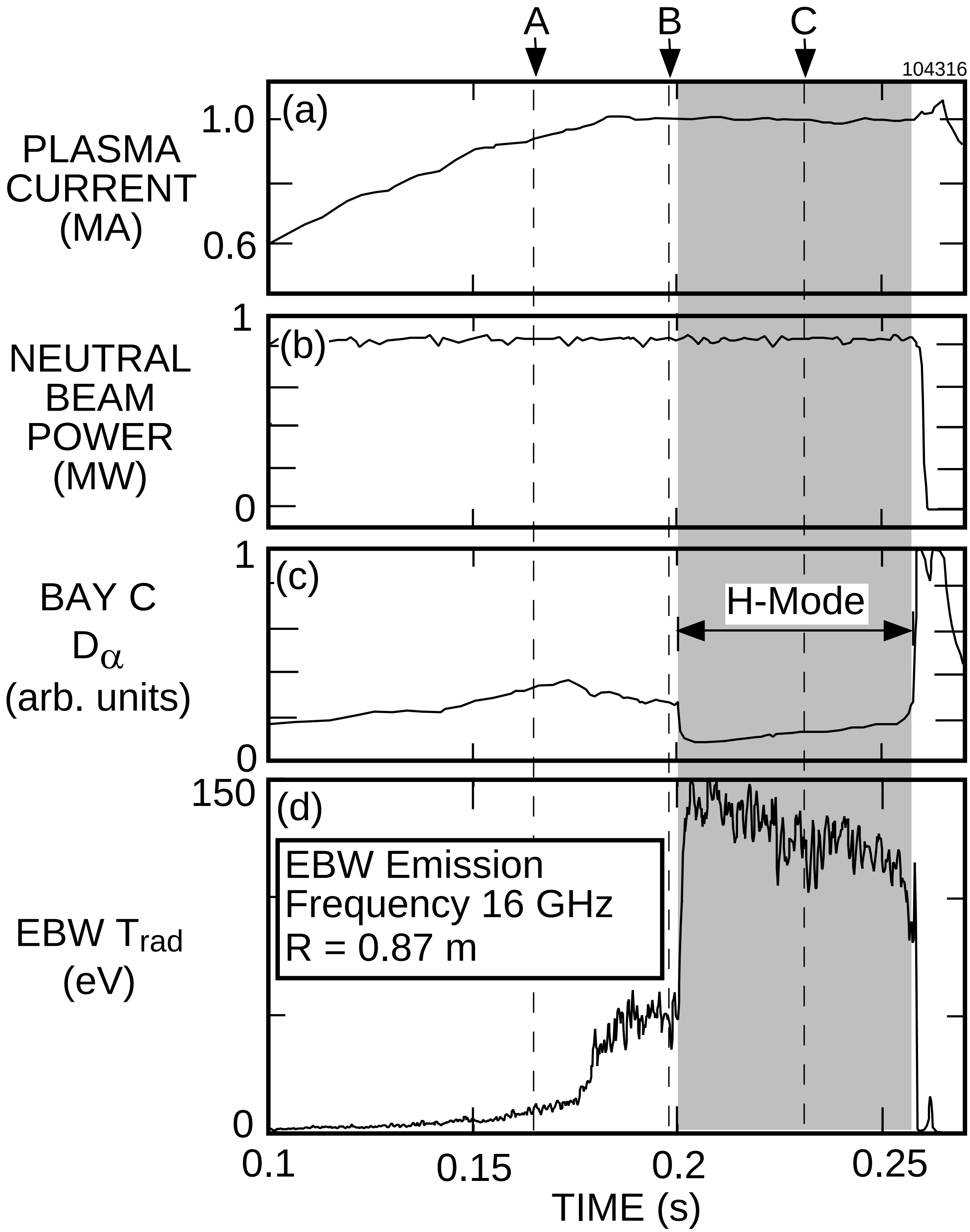

A
B
C
104316
PLASMA CURRENT (MA)
1.0
0.6
(a)
NEUTRAL BEAM POWER (MW)
1
0
(b)
BAY C D_α (arb. units)
1
0
(c)
H-Mode
EBW T_{rad} (eV)
150
0
(d)
EBW Emission
Frequency 16 GHz
R = 0.87 m
0.1
0.15
0.2
0.25
TIME (s)

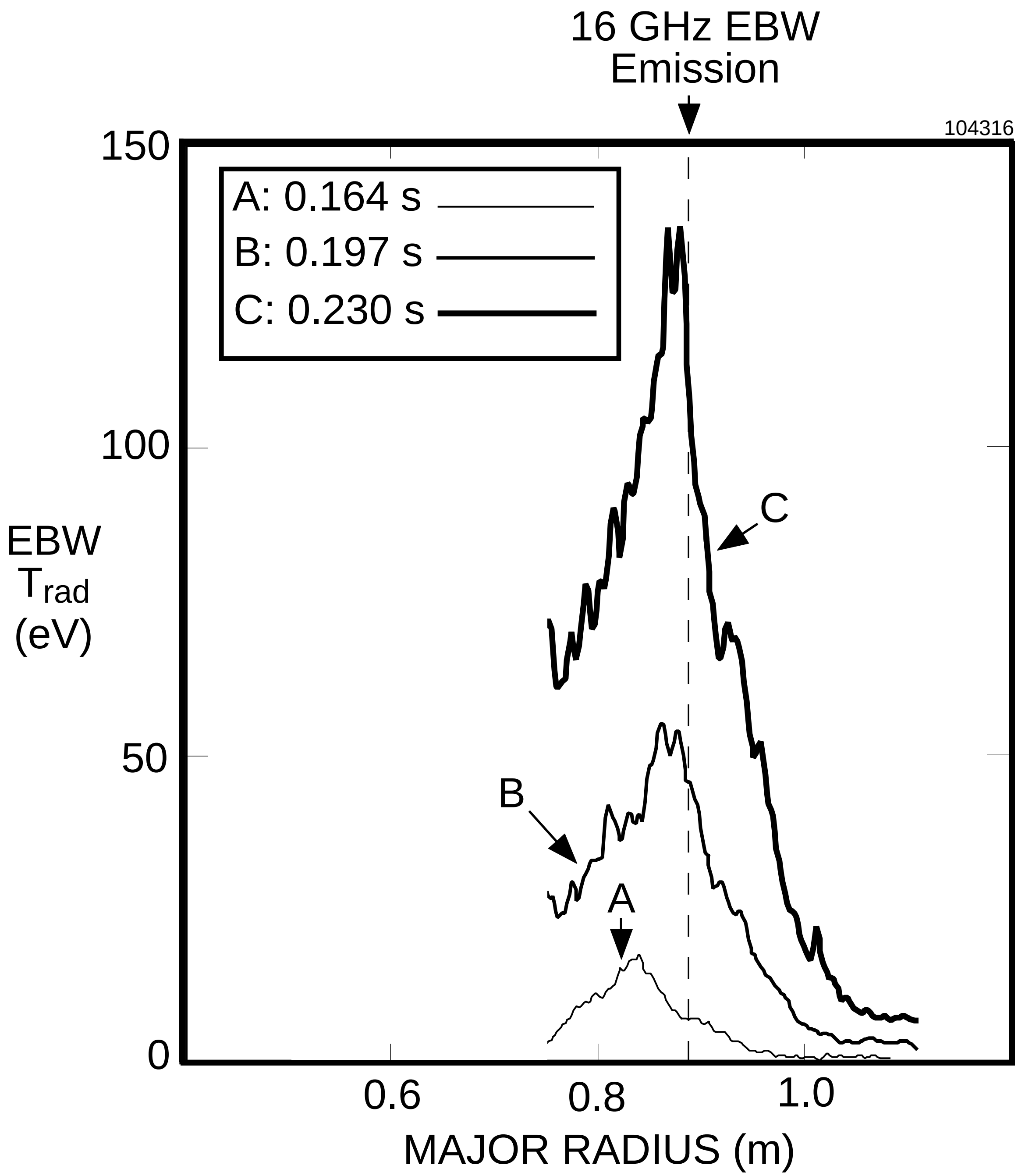

16 GHz EBW
Emission
104316
A: 0.164 s
B: 0.197 s
C: 0.230 s
150
100
50
0
EBW
Trad
(eV)
C
B
A
0.6
0.8
1.0
MAJOR RADIUS (m)

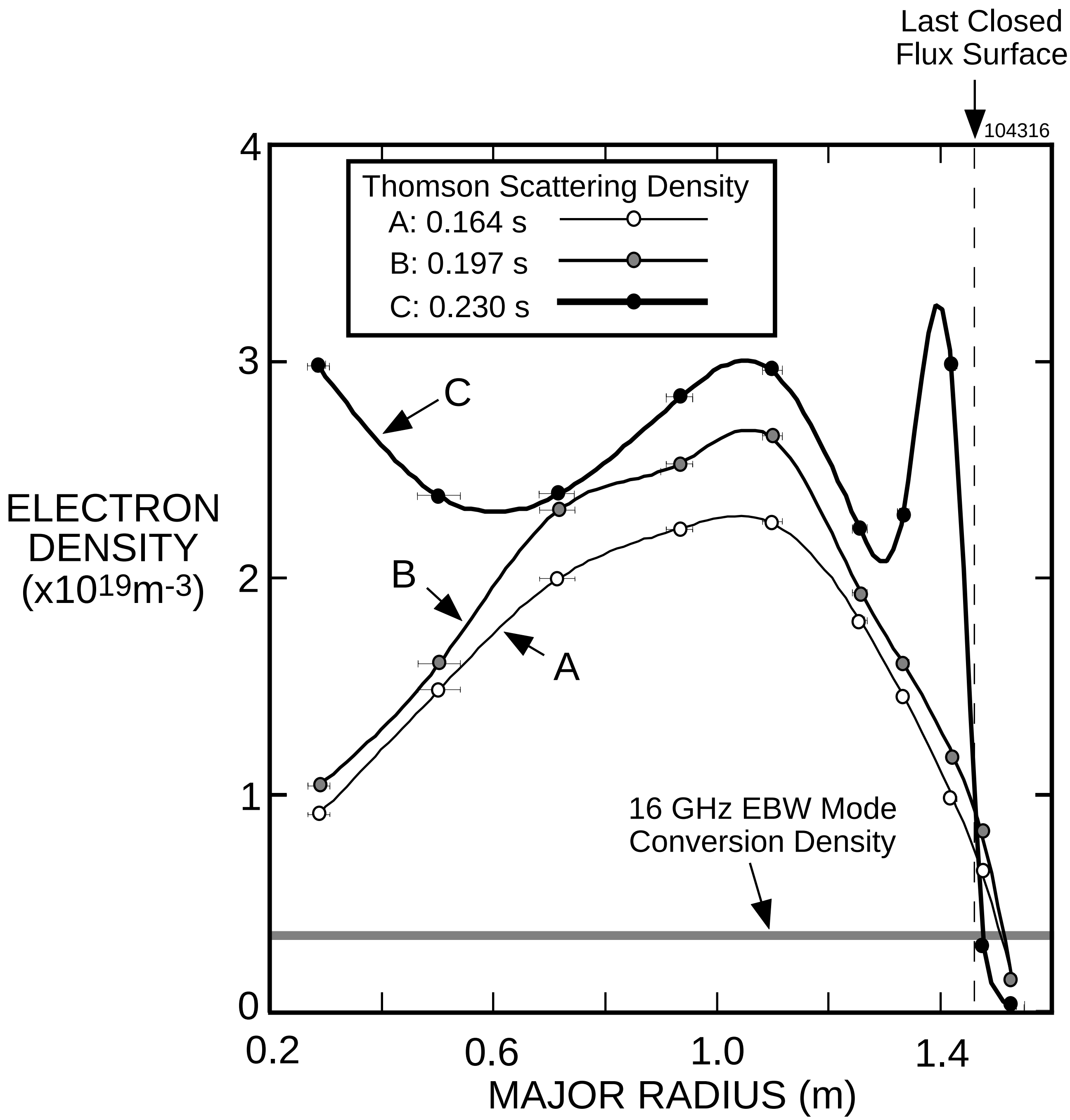

Last Closed
Flux Surface
104316
Thomson Scattering Density
A: 0.164 s
B: 0.197 s
C: 0.230 s
C
B
A
16 GHz EBW Mode
Conversion Density
ELECTRON
DENSITY
(x10^19m^-3)
4
3
2
1
0
0.2
0.6
1.0
1.4
MAJOR RADIUS (m)

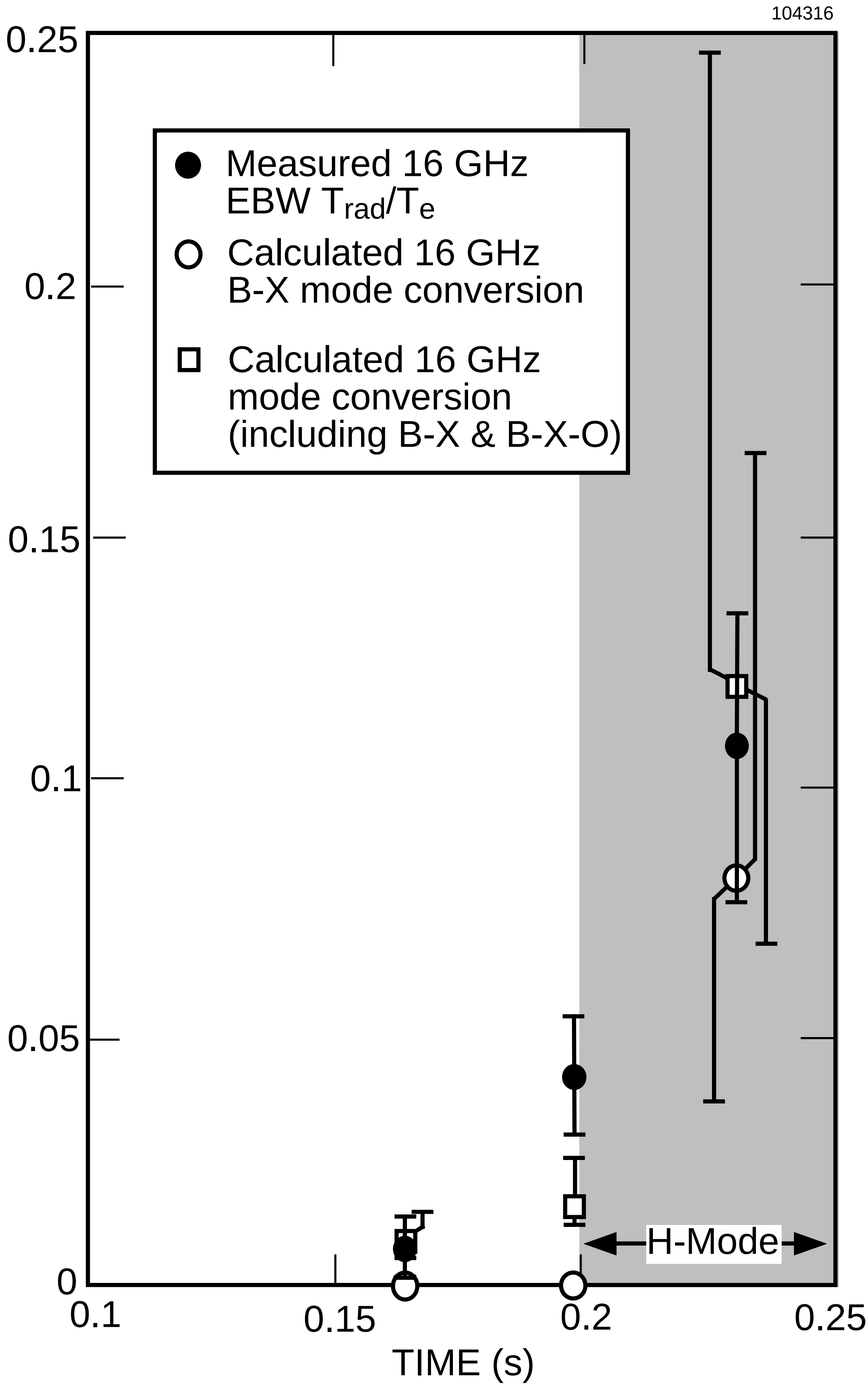

104316
Measured 16 GHz
EBW T_{rad}/T_e
Calculated 16 GHz
B-X mode conversion
Calculated 16 GHz
mode conversion
(including B-X & B-X-O)
H-Mode
0.25
0.2
0.15
0.1
0.05
0
0.1
0.15
0.2
0.25
TIME (s)

External Distribution

Plasma Research Laboratory, Australian National University, Australia
Professor I.R. Jones, Flinders University, Australia
Professor João Canalle, Instituto de Fisica DEQ/IF - UERJ, Brazil
Mr. Gerson O. Ludwig, Instituto Nacional de Pesquisas, Brazil
Dr. P.H. Sakanaka, Instituto Fisica, Brazil
The Librarian, Culham Laboratory, England
Library, R61, Rutherford Appleton Laboratory, England
Mrs. S.A. Hutchinson, JET Library, England
Professor M.N. Bussac, Ecole Polytechnique, France
Librarian, Max-Planck-Institut für Plasmaphysik, Germany
Jolan Moldvai, Reports Library, MTA KFKI-ATKI, Hungary
Dr. P. Kaw, Institute for Plasma Research, India
Ms. P.J. Pathak, Librarian, Insitute for Plasma Research, India
Ms. Clelia De Palo, Associazione EURATOM-ENEA, Italy
Dr. G. Grosso, Instituto di Fisica del Plasma, Italy
Librarian, Naka Fusion Research Establishment, JAERI, Japan
Library, Plasma Physics Laboratory, Kyoto University, Japan
Research Information Center, National Institute for Fusion Science, Japan
Dr. O. Mitarai, Kyushu Tokai University, Japan
Library, Academia Sinica, Institute of Plasma Physics, People's Republic of China
Shih-Tung Tsai, Institute of Physics, Chinese Academy of Sciences, People's Republic of China
Dr. S. Mirnov, TRINITI, Troitsk, Russian Federation, Russia
Dr. V.S. Strelkov, Kurchatov Institute, Russian Federation, Russia
Professor Peter Lukac, Katedra Fyziky Plazmy MFF UK, Mlynska dolina F-2, Komenskeho Univerzita, SK-842 15 Bratislava, Slovakia
Dr. G.S. Lee, Korea Basic Science Institute, South Korea
Mr. Dennis Bruggink, Fusion Library, University of Wisconsin, USA
Institute for Plasma Research, University of Maryland, USA
Librarian, Fusion Energy Division, Oak Ridge National Laboratory, USA
Librarian, Institute of Fusion Studies, University of Texas, USA
Librarian, Magnetic Fusion Program, Lawrence Livermore National Laboratory, USA
Library, General Atomics, USA
Plasma Physics Group, Fusion Energy Research Program, University of California at San Diego, USA
Plasma Physics Library, Columbia University, USA
Alkesh Punjabi, Center for Fusion Research and Training, Hampton University, USA
Dr. W.M. Stacey, Fusion Research Center, Georgia Institute of Technology, USA
Dr. John Willis, U.S. Department of Energy, Office of Fusion Energy Sciences, USA
Mr. Paul H. Wright, Indianapolis, Indiana, USA

The Princeton Plasma Physics Laboratory is operated
by Princeton University under contract
with the U.S. Department of Energy.

Information Services
Princeton Plasma Physics Laboratory
P.O. Box 451
Princeton, NJ 08543

Phone: 609-243-2750
Fax: 609-243-2751
e-mail: pppl_info@pppl.gov
Internet Address: http://www.pppl.gov